

Novel Defected Ground Structure and Two-Side Loading Scheme for Miniaturized Dual-Band SIW Bandpass Filter Designs

Shanshan Xu, Kaixue Ma, *Senior Member, IEEE*, Fanyi Meng, *Student Member, IEEE*, and Kiat Seng Yeo, *Senior Member, IEEE*

Abstract—This letter reports a novel back-to-back E-shaped defected ground structure (DGS) and two-side loading scheme for miniaturized dual-band substrate integrated waveguide (SIW) bandpass filter (BPF) designs. The SIW loaded by novel DGS supports evanescent-mode wave propagation below the cut-off frequency of SIW, while achieves two transmission poles at the passband and two controllable transmission zero points. Furthermore, the novel loading scheme by loading different-sized DGS resonators on two sides of SIW is proposed for dual-band BPF designs. To validate the design and analysis, a 2.4/5.2 GHz filter prototype was designed. In good agreement with theoretical results, the measured results of the dual-band filter achieve insertion losses of 3.6 and 3.1 dB, and fractional bandwidths of 5.8% and 6.45% at 2.4 and 5.2 GHz, respectively. The filter size is only 408 mil \times 420 mil.

Index Terms—Back-to-back E-shaped, bandpass filter (BPF), complementary open-loop resonator (COLR), complementary split ring resonator (CSRR), defected ground structure (DGS), dual-band filters, miniaturization, substrate integrated waveguide (SIW).

I. INTRODUCTION

SUBSTRATE integrated waveguide (SIW), synthesized on planar substrate using periodic arrays of metalized vias, has been widely used as the platform for implementing low-cost and integrated waveguide filters [1]. With the merits of low-loss and high power handling capability, filters based on SIW technology still suffer from bulky sizes compared to their microstrip counterparts [2].

To circumvent with this issue, the bandpass filters (BPFs) with forward-wave or evanescent-mode wave which can propagate below SIW cut-off frequency (f_c) by loading DGS on SIW sides, were demonstrated in [3]–[8] for filter miniaturization. In

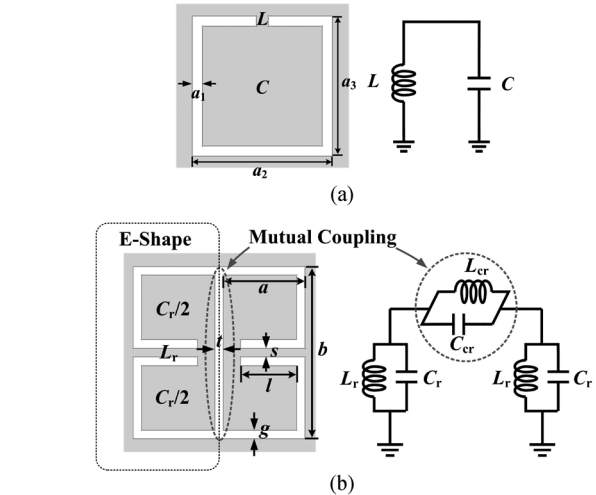


Fig. 1. Configuration and equivalent circuit of (a) the complementary open-loop resonator [10] and (b) the proposed back-to-back E-shaped DGS unit. (Grey zone: metallization; White zone: defected area).

these works, the primary investigation was leveraged on complementary split ring resonator (CSRR) [9] and complementary open-loop resonator (COLR) as in Fig. 1(a). The dual-mode and dual-band operations were demonstrated in [5] and [6], by means of loading two same- or different-sized CSRRs on the top side of SIW. To obtain lower resonant frequencies, same-sized CSRRs/COLRs were loaded on two sides of SIW in [3] and [4].

In this letter, a novel DGS shape named as back-to-back E-shaped DGS is proposed as shown in Fig. 1(b). By loading the back-to-back E-shaped DGS on either top or bottom sides of SIW, a dual-mode frequency response with two transmission zero points (ZPs) is obtained. To obtain dual-band response, a new two-side loading scheme with different-sized resonators on top and bottom sides is also proposed in this letter. To validate the concept, a dual-band (2.4/5.2 GHz) BPF is designed using Rogers RO4003 ($\epsilon_r = 3.38$, $\tan \delta = 0.0027$) with thickness of 8 mil. The fabricated filter achieves good skirt selectivity, high inter-band isolation, good spurious response, and compact size.

II. BACK-TO-BACK E-SHAPED DGS

A. Back-to-Back E-Shaped DGS

As shown in Fig. 1(b), the back-to-back E-shaped DGS is formed by two E-shapes in back-to-back orientation. From its physical configuration, the E-shaped DGSs can be modeled as

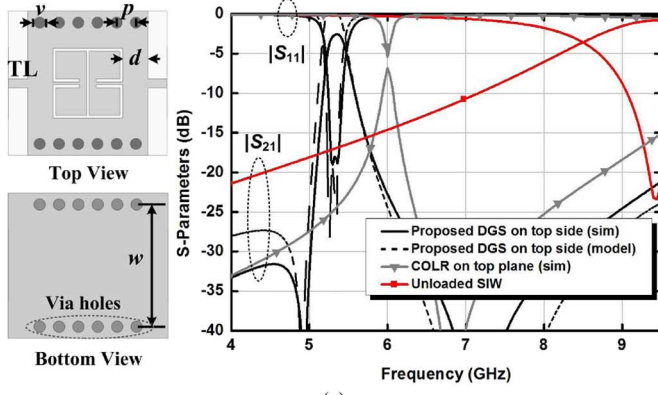


Fig. 2. Investigation of SIW loaded by back-to-back E-shaped DGS and COLR on the top side: (a) configurations and transmission responses; (b) equivalent circuit model of SIW loaded by unit back-to-back E-shaped DGS; (c) even- and odd-mode circuits. (Grey zone: metallization; White zone: defected area; Physical parameters: for SIW $d = 50$, $v = 24$, $p = 40$, $w = 372$, for single ring CSRR $a_1 = 6$, $a_2 = 145$, $a_3 = 145$, for back-to-back E-shaped DGS: $a = 70$, $b = 145$, $s = 6$, $l = 49$, $g = 6$, $t = 5$ with unit in mil; Circuit elements: $L_{ci} = 0.696$ nH, $C_{ci} = 0.692$ pF, $L_r = 0.685$ nH, $C_r = 1.68$ pF, $L_{cr} = 1.48$ nH, $C_{cr} = 0.711$ pF, and $L_d = 1.03$ nH).

LC resonators (L_r and C_r) with L_{cr} and C_{cr} denoting their mutual magnetic and electric couplings. The resonant frequencies of each E-shaped DGS are determined by a , b , g , l , and s .

B. Transmission Responses

The transmission responses are investigated by using ANSYS's HFSS V14 software packages. As shown in Fig. 2(a), the unloaded SIW has a high-pass frequency response with f_c at 9.5 GHz.

First, the SIW is loaded by COLR unit as the reference. It is observed that a transmission pole is created at 6 GHz, with one ZP at 6.9 GHz.

Secondly, the SIW is loaded by the proposed DGS in the same size. Compared to COLR, the proposed DGS achieves two transmission poles at 5.3 and 5.35 GHz as shown in Fig. 2(a), that potential benefits circuit miniaturization, enhances frequency selectivity by generating two transmission ZPs, and extends upper stopband attenuation of 20 dB to 9.5 GHz.

As shown in Fig. 2(b), the equivalent circuit models are developed for the proposed filter. The two sides of SIW are treated as a two-wire transmission lines while the via arrays are modeled as inductors L_d [5]. The input coupling comprises of both magnetic and electric couplings that are represented as L_{ci} and

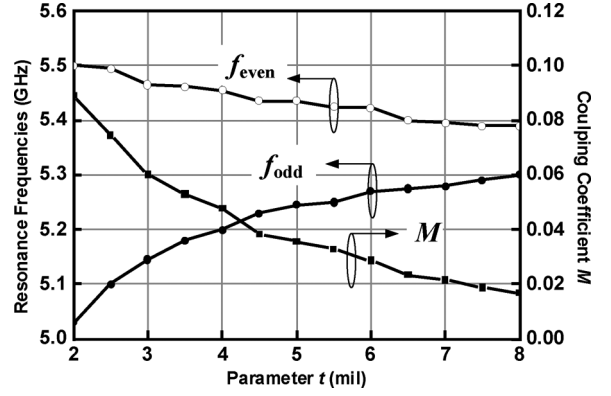


Fig. 3. EM investigation of even, odd frequencies and coupling coefficient versus parameter t . (Parameters of structure in Fig. 1 given in caption of Fig. 2).

C_{ci} . In Fig. 2(a), the simulation results of the circuit model are well agreed with EM simulation results. Even- and odd-mode analysis is adopted to study the resonant properties. Using circuits in Fig. 2(c), the odd-/even-mode input admittances are derived as in (1) and (2)

$$Y_{ino} = -\frac{j}{\omega L_d} + \frac{\left(-\frac{j}{\omega L_{ci}} + j\omega C_{ci}\right) \left[-\frac{j}{\omega} \left(\frac{1}{L_r} + \frac{2}{L_{cr}}\right) + j\omega(C_r + 2C_{cr})\right]}{-\frac{j}{\omega} \left(\frac{1}{L_{ci}} + \frac{1}{L_r} + \frac{2}{L_{cr}}\right) + j\omega(C_{ci} + C_r + 2C_{cr})} \quad (1)$$

$$Y_{ine} = -\frac{j}{\omega L_d} + \frac{\left(-\frac{j}{\omega L_{ci}} + j\omega C_{ci}\right) \left(-\frac{j}{\omega L_r} + j\omega C_r\right)}{-\frac{j}{\omega} \left(\frac{1}{L_{ci}} + \frac{1}{L_r}\right) + j\omega(C_{ci} + C_r)} \quad (2)$$

The odd- and even-mode transmission poles are located when Y_{ino} and Y_{ine} approaches infinity

$$f_{odd} = \frac{\sqrt{L_r L_{cr} + L_{ci} L_{cr} + 2L_{ci} L_r}}{2\pi \sqrt{L_{ci} L_r L_{cr} (C_{ci} + C_r + 2C_{cr})}}, \quad (3)$$

$$f_{odd} = \frac{\sqrt{L_r + L_{ci}}}{2\pi \sqrt{L_{ci} L_r (C_{ci} + C_r)}} \quad (4)$$

where only odd-mode resonant frequency f_{odd} is influenced by the mutual coupling elements L_{cr} and C_{cr} . It is investigated by using EM simulation as the results given in Fig. 3 by varying parameter t and extracting the coupling coefficients M as

$$M = \frac{|f_{odd}^2 - f_{even}^2|}{f_{odd}^2 + f_{even}^2} \quad (5)$$

It is verified that f_{odd} is much more sensitive to the variation of k while f_{even} has negligible frequency shift. On the other hand, the transmission ZPs are determined using $Y_{ine} = Y_{ino}$ [11]

$$f_{ZP1} = \frac{1}{2\pi \sqrt{L_{ci} C_{ci}}}, \quad f_{ZP2} = \frac{1}{2\pi \sqrt{L_{ci} C_{cr}}} \quad (6)$$

which are controlled by the input and mutual couplings.

Based on the EM extraction parameters, the single band second-order filter is designed. With a targeted FBW, the external quality factor (Q_e) and the coupling coefficient (M_{12}) between two DGS resonators are determined through the circuit

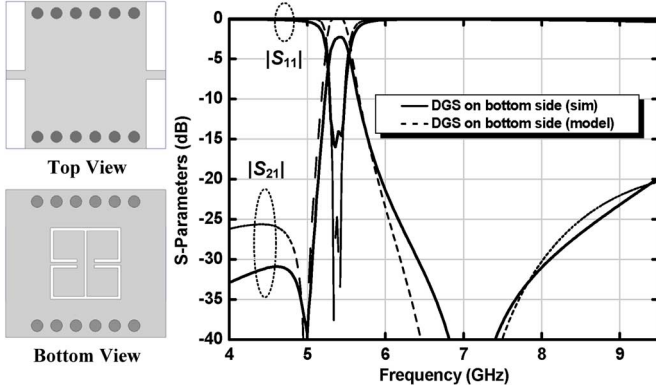


Fig. 4. A second-order BPF design based on SIW loaded by back-to-back E-shaped DGS unit on the bottom side. (Physical parameters: same as the caption of Fig. 2 with $d = 52.5$ mil; Circuit elements: $L_{ci} = 0.686$ nH, $C_{ci} = 0.772$ pF, $L_r = 0.665$ nH, $C_r = 1.58$ pF, $L_{cr} = 1.48$ nH, $C_{cr} = 0.691$ pF, and $L_d = 1.33$ nH).

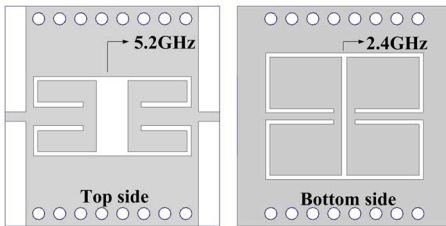


Fig. 5. The 2.4/5.2 GHz dual-band SIW BPF. (Physical parameters: Top side $s = 35$, $t = 60$, $a = 120$, $b = 152$, $g = 8$, $l87$, and $d = 14$; Bottom side $s = 14$, $t = 10$, $a = 145$, $b = 242$, $g = 8$, and $l = 122$).

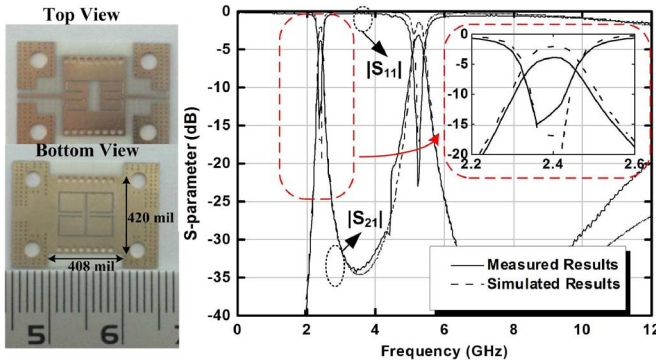


Fig. 6. Photographs, simulated and measured S-parameters of the proposed filter.

element of the Chebyshev low-pass filter prototype [11]. The example DGS filter operated in 5.2 GHz loaded on the bottom side of SIW is given in Fig. 4.

III. DUAL-BAND BANDPASS FILTER PROTOTYPE

As shown in Fig. 5, a dual-band BPF is designed by loading DGS resonators on both top and bottom sides. A back-to-back E-shaped DGS filter on top side for the 5.2 GHz band and a DGS on bottom side for the 2.4 GHz band are proposed. The 2.4 GHz filter is designed first with fractional bandwidth (FBW) of 5.8%. The coupling coefficient is calculated as $Q_e = 12.97$ and $M_{12} = 0.089$. With 2.4 GHz resonator loaded on the bottom side, the 5.2 GHz passband is designed on the top side with FBW of 6.5%, the coupling matrix is generated as $Q_e = 14.54$ and $M_{12} = 0.079$. Since the frequency 5.2 GHz is 2.17 times of that of the 2.4 GHz band, the size of the 5.2 GHz BB-E-shaped

DGS is much smaller than that of the 2.4 GHz one. As a result, 5.2 GHz filter has relatively less effect on the 2.4 GHz filter. The dual-band filter can be designed by EM optimization of the stacked 5.2 GHz filter on top and 2.4 GHz on bottom. Thus, compared to parallel loading two different-sized resonators on the same side [6], the size of proposed dual-band filter can be reduced by half.

Fig. 6 shows the fabricated dual-band filter with a compact size of 408 mil \times 420 mil (i.e., $0.152\lambda_g \times 0.156\lambda_g$, λ_g is the 2.4 GHz guided wavelength). The measured results agree with the EM simulation result. For the 2.4 GHz band, the insertion loss is 3.6 dB with a 3 dB FBW of 5.8%. For the 5.2 GHz band, the insertion loss is 3.1 dB with FBW of 6.45%. The return losses are better than 15 dB in both passbands. The designed dual-band filter shows a sharp roll-off and high inter-band isolation better than 34 dB due to the generation of two transmission ZPs. The upper stopband with more than 20 dB attenuation extends to 12 GHz.

IV. CONCLUSION

In this letter, the back-to-back E-shaped DGS and the two-side loading scheme of different-sized DGSs on top and bottom sides of SIW are proposed for miniaturized dual-band filter designs. Based on the analysis and investigations, a 2.4/5.2 GHz BPF was designed and verified experimentally. It is noted that the proposed back-to-back E-shaped DGS for SIW and loading scheme can be extended for miniaturized multi-band components.

REFERENCES

- [1] S. Wong, K. Wang, Z.-N. Chen, and Q.-X. Chu, "Design of millimeter-wave bandpass filter using electric coupling of substrate integrated waveguide (SIW)," *IEEE Microw. Wireless Compon. Lett.*, vol. 24, pp. 26–28, Dec. 2014.
- [2] K. Ma, J.-G. Ma, K. S. Yeo, and M. A. Do, "A compact size coupling controllable filter with separate electric and magnetic coupling paths," *IEEE Trans. Microw. Theory Tech.*, vol. 54, pp. 1113–1119, Mar. 2006.
- [3] L. Huang, I. D. Robertson, and N. Yuan, "Substrate integrated waveguide filters with face-to-face broadside-coupled complementary split ring resonators," in *Proc. Eur. Microw. Conf. (EuMC)*, 2013, pp. 29–32.
- [4] W.-Y. Park and S. Lim, "Miniaturized substrate integrated waveguide (SIW) bandpass filter loaded with double-sided-complementary split ring resonators (DS-CSRRs)," in *Proc. Eur. Microw. Conf. (EuMC)*, 2011, pp. 740–743.
- [5] Y. Dong, T. Yang, and T. Itoh, "Substrate integrated waveguide loaded by complementary split-ring resonators and its applications to miniaturized waveguide filters," *IEEE Trans. Microw. Theory Tech.*, vol. 57, pp. 2211–2223, Aug. 2009.
- [6] Y. Dong and T. Itoh, "Miniaturized dual-band substrate integrated waveguide filters using complementary split-ring resonators," in *IEEE MTT-S Int. Dig.*, 2011, pp. 1–4.
- [7] Q.-L. Zhang, W.-Y. Yin, and S. He, "Evanescent-mode substrate integrated waveguide (SIW) filters implemented with complementary split ring resonators," *Progress Electrom. Res.*, vol. 111, pp. 419–432, 2011.
- [8] W. Shen, W.-Y. Yin, and X.-W. Sun, "Compact substrate integrated waveguide (SIW) filter with defected ground structure," *IEEE Microw. Wireless Compon. Lett.*, vol. 21, pp. 83–85, Feb. 2011.
- [9] F. Falcone *et al.*, "Effective negative- ϵ stopband microstrip lines based on complementary split ring resonators," *IEEE Microw. Wireless Compon. Lett.*, vol. 14, pp. 280–282, Jun. 2004.
- [10] J. Baena *et al.*, "Equivalent-circuit models for split-ring resonators and complementary split-ring resonators coupled to planar transmission lines," *IEEE Trans. Microw. Theory Tech.*, vol. 16, pp. 543–545, Oct. 2006.
- [11] J. S. Hong and M. J. Lancaster, *Microstrip Filter for RF/Microwave Application*. New York: Wiley, 2001.